A Measure of Similarity Between Images Based on the Codispersion Coefficient

*Silvia M. Ojeda [1] Ronny O. Vallejos [2] and Pedro W. Lamberti [1]

[1] Facultad de Matemática, Astronomía y Física, Universidad Nacional de Córdoba
Haya de la Torre y Medina Allende S/N, CP 5000, Córdoba, Argentina

[2] Departamento de Matemática, Universidad Técnica Federico Santa María.
Casilla 110-V, Valparaíso, Chile.

Abstract

We propose to use the codispersion coefficient to define a measure of similarity between images. This coefficient has been widely used in spatial statistics to quantify the association between two spatial processes, and here we explore its capabilities in an image processing context. It is mathematically simple to compute and possesses good statistical properties. The new measure takes into account the spatial association in a specific direction h between a degraded image and the original unmodified image. Three applications are developed to illustrate the capabilities of our proposal. The defined measure captures the spatial association that is produced by fitting AR-2D processes with different window sizes. It is able to distinguish the levels of similarity between two images for specific directions in two-dimensional space. Finally, it detects stochastic resonance when an image is transmitted by a nonlinear device.

Key words: Image quality index, codispersion coefficient, AR-2D processes, stochastic resonance.

*Corresponding author: S. Ojeda: ojeda@mate.uncor.edu

1 Introduction

Image quality measures play an important role in many different fields and applications. The criteria for quantifying the dissimilarity between two images have been extensively studied in the literature [1], [2]. Specifically, a measure called the structural similarity (SSIM) index has been proposed as a measure of image quality [3], and later, an application of SSIM to stochastic resonance was studied in the context of nonlinear image transmission [4]. Additional information about image quality measures and dissimilarity between images can be found in [5], [6].

In the context of spatial sequences, an initial study on the association between two spatial processes was performed in [7]. Subsequently, a coefficient was proposed that is a corrected version of the correlation coefficient [8]. In contrast, the codispersion coefficient that was first introduced by Matheron [9] was used to quantify the spatial association in many different applications. This coefficient is a generalization of the classical variogram commonly used to describe the association structure of a single process. Three decades later, the codispersion coefficient received attention from a theoretical point of view [10]. Recently, the coefficient was adapted to the case where the processes are defined on the real line. In that case, the codispersion captures the comovement between the trajectories of two stochastic processes [11].

In this work, we propose to use the codispersion coefficient to define a measure of similarity between two images in a specific direction h, in the same way as the cross-correlation function is used in time series. Three applications with synthetic and real data will be described to obtain better insight into the performance of the proposed measure in practice.

2 The Codispersion Coefficient

Consider two weakly stationary processes, $X(s)$ and $Y(s)$, $s \in D \subset \mathbb{Z}^d$. The cross-variogram between $X(s)$ and $Y(s)$ is defined as the following:

$$\gamma(h) = \mathbb{E}[X(s+h) - X(s)][Y(s+h) - Y(s)], \tag{1}$$

such that $s, s+h \in D$. The codispersion coefficient is a normalized version of (1) given by

$$\rho(h) = \frac{\gamma(h)}{\sqrt{V_X(h)V_Y(h)}}, \tag{2}$$

where $V_X(h) = \mathbb{E}[X(s+h) - X(s)]^2$ and similarly for $V_Y(h)$. It is obvious that $|\rho(h)| \leq 1$. For cases in which $X(s)$ and $Y(s)$ are parametric (spatial ARMA) models defined on the plane, explicit expressions for $\rho(h)$ have been proposed in the literature [10]. Also, under regularity conditions, the sample codispersion coefficient defined by

$$\widehat{\rho}(h) = \frac{\sum_{s,s+h\in D'} a_s b_s}{\sqrt{\widehat{V}_X(h)\widehat{V}_Y(h)}} \tag{3}$$

with $s = (s_1, s_2)$, $h = (h_1, h_2)$, $D' \subseteq D$, $\#(D') < \infty$, $a_s = X(s_1 + h_1, s_2 + h_2) - X(s_1, s_2)$, $b_s = Y(s_1+h_1, s_2+h_2) - Y(s_1, s_2)$, $\widehat{V}_X(h) = \sum_{s,s+h\in D'} a_s^2$, and $\widehat{V}_Y(h) = \sum_{s,s+h\in D'} b_s^2$ is consistent and asymptotically normal [10]. These statistical properties allow us to construct confidence intervals and hypothesis tests for the coefficient [11].

This coefficient has been useful in many different applications. For example, the spatial covariation of Azotobacter abundance and soil properties was analyzed in [12]. Rukhin and Vallejos [10] computed the codispersion coefficient from images related to the effects of the dispersion and concentration of one retardant to improve the flammability properties of polymers. In [13] the codispersion coefficient was used to quantify the spatial and temporal patterns of Lolium rigidum-Avena sterilis mixed populations in a cereal field.

3 Image Quality Assessment

Given two sequences $\boldsymbol{x} = \{X(s_i) : i = 1, 2, \ldots, n\}$ and $\boldsymbol{y} = \{Y(s_i) : i = 1, 2, \ldots, n\}$, in [3] it was proposed that the index SSIM be defined by the following equation:

$$Q = \frac{4S_{XY}\overline{X}\,\overline{Y}}{(S_X^2 + S_y^2)[\overline{X}^2 + \overline{Y}^2]} = \frac{S_{XY}}{S_X S_Y} \cdot \frac{2\overline{X}\,\overline{Y}}{\overline{X}^2 + \overline{Y}^2} \cdot \frac{2S_X S_Y}{S_X^2 + S_Y^2} = C \cdot M \cdot V, \tag{4}$$

where $C = \frac{S_{XY}}{S_X S_Y}$ models the linear correlation between $\boldsymbol{x}$ and $\boldsymbol{y}$, $M = \frac{2\overline{X}\,\overline{Y}}{\overline{X}^2+\overline{Y}^2}$ measures the similarity between the sample means (luminance) of $\boldsymbol{x}$ and $\boldsymbol{y}$, and $V = \frac{2S_X S_Y}{S_X^2+S_Y^2}$ measures the similarity related to the contrast between the images. Coefficient Q is defined as a function of

the correlation coefficient; hence, it is able to capture only the linear association between $\boldsymbol{x}$ and $\boldsymbol{y}$ but is unable to account for other types of relationships between these sequences, for example, the spatial association in a specific direction h. This disadvantage of Q led us to consider a new proposal to address image quality assessment, namely, the CQ index, which is defined as:

$$CQ(h) = \widehat{\rho}(h) \cdot M \cdot V, \tag{5}$$

where M and V are defined as in (4). Notice from (5) that, instead of using the correlation coefficient, we use the codispersion index to account for the spatial association between sequences $\boldsymbol{x}$ and $\boldsymbol{y}$ in the direction h. We recall that $\widehat{\rho}(h)$ does not necessarily capture similarity that is related to the patterns or shapes that are present in the images; instead, it captures the spatial dependence between sequences $\boldsymbol{x}$ and $\boldsymbol{y}$ for a given lag distance h.

4 Applications to Images

We developed three examples in different scenarios to explore some features of the CQ index. Four real images were used in this section, Lenna, Mandrill, Girl and Wheat, all taken from the USC-SIPI image database [14].

4.1 Similarity Between Images Generated by AR-2D Models

In this experiment, we show that the CQ index has the capability of capturing the spatial association level between two images. First, we consider an original image and then we apply the algorithm that was developed in [15] to obtain an image that is generated by a two-dimensional autoregressive (AR-2D) process. This algorithm consists of locally fitting an AR-2D model to the original image, which is divided into small regions. An AR-2D model is fitted to each of these regions so that a new image is generated, putting together all of the images that were generated by fitting the local AR-2D models to the original image. In each case, a least squares estimation for the parameters of the AR-2D model was considered. The fitted autoregressive image strongly depends on the size of the moving window. Indeed, a small window size is associated with a large number of AR models that were fitted to the original image (see [15]). This process produces a

better local approximation, and hence, the patterns in the fitted image are very well represented. However, when the window size is large, the fitted image is a poor representation of the original image (even if there are not visually detectable differences). In [15], the residual images were analyzed to construct an image segmentation algorithm. Here, we compare the indices CQ and Q to quantify the similarity between the original and each of the new images that were generated by the algorithm.

Figure 1(a) shows an original image of size 512×512 (Lenna). Images (b)-(i) were obtained by using the algorithm developed in [15] with a moving window size of 4×4; 8×8; 16×16; 32×32; 64×64; 128×128; 256×256, and 512×512, respectively. Visually, there is no difference between the original image and any of the images generated by the algorithm; however, the residual images reveal significant differences (see for example, images (j), (k) and (l) in Figure 1). More details about residual images in image segmentation can be found in [15].

Table 1 shows that the maximum value of the CQ index corresponds to the smallest (optimal) moving window size (4×4). This is in agreement with the results found in [15] (based on the mean square error) and indicates that an image that is generated with a small window size is more spatially associated with the original image than with other images that were generated with bigger window sizes. However, in this example, the Q index is unable to capture the dependence of the fitted image on the window size. Indeed, while the window size varies, Q shows a non-pattern performance. Similar results were obtained for a large set of images, all taken from the USC-SIPI image database [14]. A full comparative study between both measures considering others degradation schemes will be a topic to be tackle in future research.

Note from the Table 1, the similarity between C and Q, as well as $\widehat{\rho}(1,1)$ and $CQ(1,1)$. This behavior results from the fact that there are not significant differences in the luminance and contrast between the original and fitted images. As a result, in (4) and (5), M and V are close to 1. This pattern may not happen for other images.

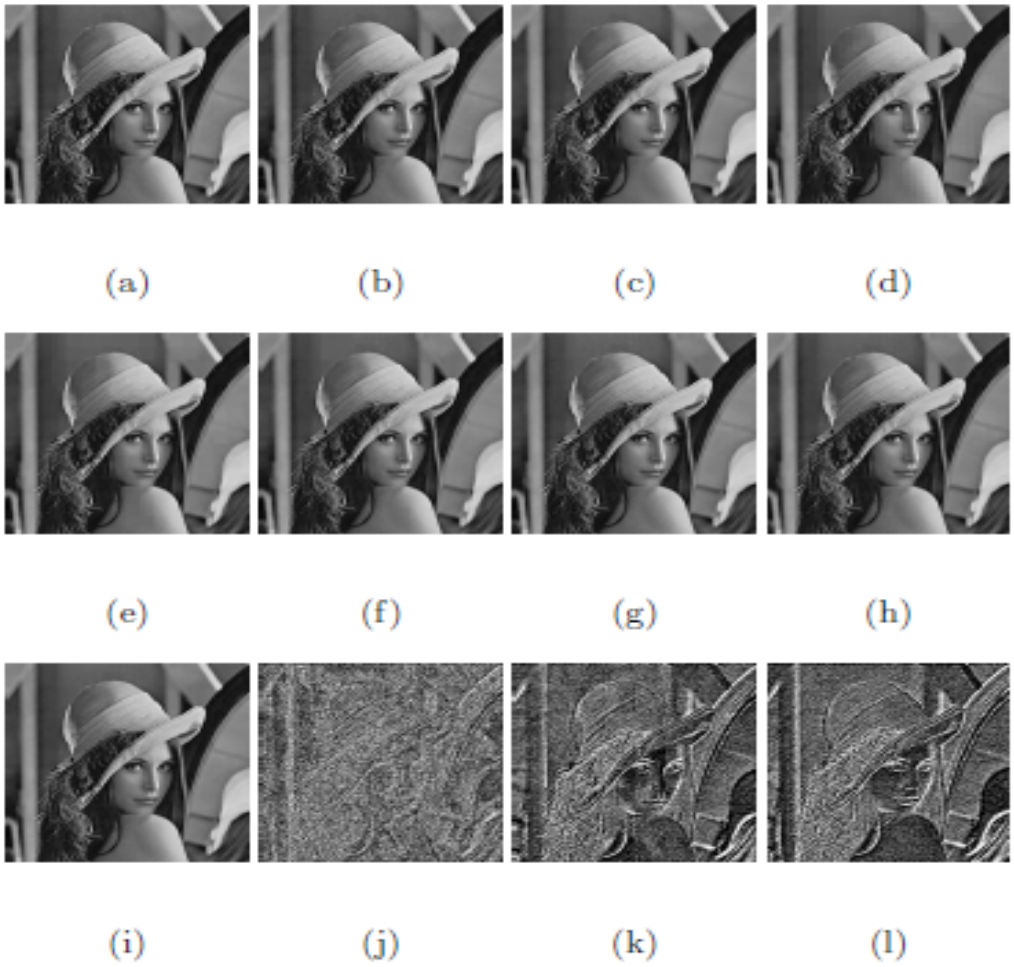

Figure 1: (a) Original image (Lenna); (b)-(i) Images generated by an AR-2D models with window sizes of 4×4; 8×8; 16×16; 32×32; 64×64; 128×128; 256×256, and 512×512, respectively; (j), (k) and (l) are the residual images for (b), (f) and (i) respectively.

Table 1: C, Q, $\widehat{\rho}(1,1)$ and $CQ(1,1)$ for different window sizes.

Window Size	C	Q	$\widehat{\rho}(1,1)$	$CQ(1,1)$
4×4	0.9788	0.9787	0.6197	0.6196
8×8	0.9754	0.9751	0.5757	0.5755
16×16	0.9777	0.9773	0.6076	0.6073
32×32	0.9777	0.9772	0.6056	0.6053
64×64	0.9776	0.9751	0.6015	0.5999
128×128	0.9771	0.9766	0.5885	0.5882
256×256	0.9768	0.9758	0.5821	0.5815
512×512	0.9766	0.9763	0.5788	0.5786

4.2 Measuring Similarity in different directions

The aim of this section is to show the capacity of CQ to capture different levels of similarity between two images, considering different directions in the images. We work over three images, Lenna, Mandrill, and Girl (from the database [14]). The same algorithm used in the previous section was considered to fit an AR-2D process to the images. We generated the best and the worst fit for each image, and then we calculated the indices Q and CQ between the fitted and original images. In the computation of CQ, three different directions were used: $h = (1,0)$, $h = (0,1)$ and $h = (1,1)$. Table 2 shows that CQ varies for different directions, and the largest values of the coefficient are associated with the window size that produces the best fit (4×4), whereas Q yields the same value for the examined directions exhibiting its independence of h.

In general, the selection of h is of great importance. In some cases there is a special interest in a particular direction h in which $CQ(h)$ can be computed. However, in other circumstances there is no prior knowledge regarding the best value of h. In practical situations, we suggest to use the codispersion map in the same way as the variogram map is used in spatial statistics (see [16]). This is a diagram in which the codispersion coefficient is computed over a grid including many selected directions on the plane, providing a useful tool to look (for example) for the largest and smallest values of the spatial association between the processes.

Table 2: Q and CQ for three different lags considering the smallest and the largest window size.

Image	Window Size	Q	CQ		
			$CQ(1,0)$	$CQ(0,1)$	$CQ(1,1)$
Lenna	4×4	0.9787	0.3170	0.5368	0.6196
	512×512	0.9763	0.3009	0.5078	0.5786
Mandrill	4×4	0.9196	0.6464	0.4184	0.6884
	512×512	0.8706	0.3999	0.0861	0.4586
Girl	4×4	0.9617	0.4538	0.3786	0.5481
	256×256	0.9707	0.4234	0.3127	0.5086

4.3 Stochastic Resonance

In this section, we use and confront Q with the indices $\widehat{\rho}(h)$ and $CQ(h)$ to assess image transmission by a nonlinear device in the presence of noise. Specifically, we study the stochastic resonance effect, where noise can play an important role when constructing an image that is transmitted by a nonlinear sensor. An input image $\boldsymbol{x}$ is contaminated independently by an additive noise $\boldsymbol{n}$ that has a zero mean and standard deviation σ. The noise image $\boldsymbol{x} + \boldsymbol{n}$ is then transmitted by a nonlinear device, which is defined as the following:

$$\boldsymbol{y} = g(\boldsymbol{x} + \boldsymbol{n}). \tag{6}$$

We consider $g(\cdot)$ as a sensor that remains linear for small positive intensities but that saturates when the intensities exceed a level θ [4], as follows:

$$g(u) = \begin{cases} 0, & \text{for } u < 0, \\ u, & \text{for } 0 \leq u \leq \theta, \\ \theta, & \text{for } u > \theta. \end{cases} \tag{7}$$

An experiment with a real data set was performed considering an image that has intensities in $[0, 1]$ and a saturation level of $\theta < 1$. The image shown in Figure 3 (a) was contaminated by a zero mean Gaussian noise $\boldsymbol{n}$. Using (7), the image was transmitted considering a threshold $\theta = 0.2$. The coefficients $\widehat{\rho}(h)$, Q and $CQ(h)$ were then computed for different values of σ that belong to the interval $[0, 3]$. The results are shown in Figure 2. We see from Figure 2 that all of the coefficients achieve their best values at a nonzero level of σ. The maximum values of $\widehat{\rho}(h)$, Q and $CQ(h)$ are attained at $\sigma = 0.26$, $\sigma = 0.32$ and $\sigma = 0.24$, respectively. This result reflects the

possibility of a constructive action of the noise to improve the image transmission in the presence of a strong saturation of the sensor.

A visual appreciation regarding the impact of noise on the input-output similarity can be obtained from Figure 3. In (Figure 3 (c)-(d)), the reconstructive effect produced by the Gaussian noise can be observed.

The results presented in Section 4 are not restrictive to the images that are treated in this paper. There is a large set of images for which the experiments developed in this article can be replicated.

5 Conclusion

This paper proposes a measure of similarity between images based on the codispersion coefficient and illustrates its capabilities in an image processing framework. This new index, called CQ, can quantify the similarity between images that is generated using a local approximation of AR-2D processes with different window sizes. Moreover, CQ captures different levels of spatial similarity between two images by considering different directions in two-dimensional space. Similarly to other measures of association, CQ detects stochastic resonance when the original image has been additively contaminated with Gaussian noise. In the light of the examples presented in this article, we suggest in practice to use index CQ as a complement of other quality measures, to not disregard possible spatial association between the processes.

Acknowledgment

R. Vallejos was partially supported by UTFSM grant 12.10.03, CCTVal FB 0821, under grant FB/01RV/11, and Fondecyt grant 1120048, Chile. P. Lamberti is a member of CONICET, Argentina. S. Ojeda and P. Lamberti thank SeCyT-UNC for financial assistance. The authors also acknowledge the suggestions from two anonymous referees, an associate editor and the editor of JEI that improved the manuscript.

References

[1] J. B. Martens and L. Meesters, "Image Dissimilarity," *Signal Process.,* vol. 70, pp. 155-176, 1998.

[2] A. M. Eskicioglu and P. S. Fisher, "Image quality measures and their performance," *IEEE Trans. Commun.,* vol. 43, pp. 2559-2565, 1995.

[3] Z. Wang and A. B. Bovik, "A universal image quality index," *IEEE Signal Processing Letters,* vol. 9, pp. 81-84, 2002.

[4] D. Rousseau, A. Delahaies and F. François-Blondeau, "Structural similarity measure to assess improvement by noise in nonlinear image transmission," *IEEE Signal Processing Letters.,* vol. 17, 36-39, Jan. 2010.

[5] T. N. Pappas and R. J. Safranek, "Percentual criteria for image quality evaluation," in *Handbook of Image Video Processing,* A. C. Bovik, Ed. New-York: Academic, 2000.

[6] Z. Wang, A. B. Bovik, H. R. Sheikh and E. P. Simoncelli, "Image quality assessment: From error visibility to structural similarity," *IEEE Trans. Image Process.,* vol. 13, pp. 600-612, 2004.

[7] D. TjΦstheim, "A measure of association for spatial variables," *Biometrika,* vol. 65, pp. 109-114, 1978.

[8] P. Clifford, S. Richardson and D. Hémon, "Assessing the significance of the correlation between two spatial processes," *Biometrics* vol. 45, pp. 123-134, 1989.

[9] G. Matheron, *Les Variables Régionalisées et leur Estimation* Paris: Masson, 1965.

[10] A. Rukhin, and R. Vallejos, "Codispersion coefficient for spatial and temporal series," *Statistics and Probability Letters,* vol. 78, pp. 1290-1300, 2008.

[11] R. Vallejos, "Assessing the association between two spatial or temporal sequences," *Journal of Applied Statistics,* vol. 35, pp. 1323-1343, 2008.

[12] R. J. Barnes, S. J. Baxter and R. M. Lark, "Spatial covariation of Azotobacter abundance and soil properties: A case study using the wavelet transform," *Soil Biology & Biochemistry* vol. 39, pp. 295-310, 2007.

[13] J. M. Blanco-Moreno, L. Chamorro and F. X. Sanz, "Spatial and temporal patterns of Lolium rigidum-Avena sterilis mixed populations in a cereal field," *European Weed Research Society Weed Research* vol. 46- pp. 207-218, 2006.

[14] USC-SIPI image database. http://sipi.usc.edu/database/.

[15] S. Ojeda, R. Vallejos and O. Bustos, "A New Image Segmentation Algorithm with Applications to Image Inpainting," *Computational Statistics & Data Analysis,* vol. 54, pp. 2082-2093, 2010.

[16] R. Goovaerts, *Geostatistics for natural resources evaluation* New York: Oxford University Press, 1997.

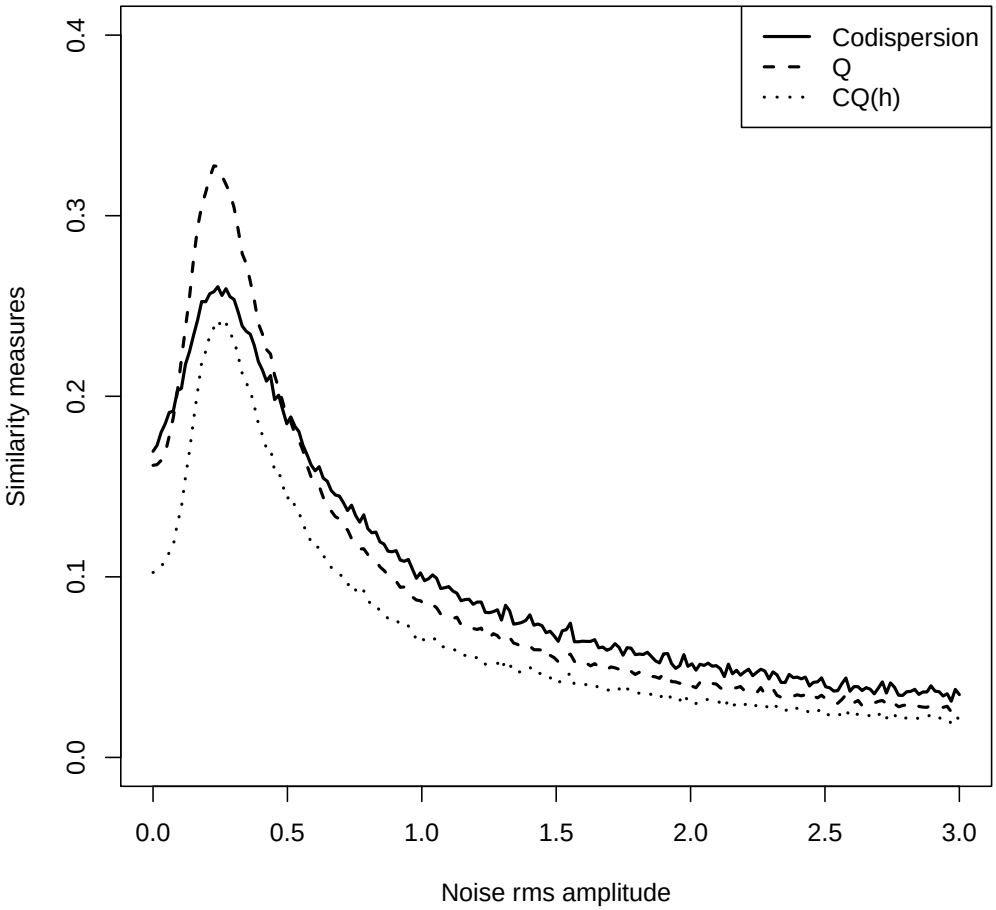

Figure 2: For the transmission by (7) with saturation level $\theta = 0.2$ of the gray level image $\boldsymbol{x}$ of Figure 3 (a) as a function of the rms amplitude σ of the zero mean Gaussian noise $\boldsymbol{n}$ in (6). The plots are $\widehat{\rho}(h)$, Q and $CQ(h)$ versus σ, for $(h_1, h_2) = (1, 1)$.

(a) (b) (c) (d) (e)

Figure 3: (a) Original input image $\boldsymbol{x}$ (Wheat); (b)-(e) output image $\boldsymbol{y}$ with $\theta = 0.2$; (b) output $\boldsymbol{y}$ with no contamination ($\sigma = 0$); (c) output $\boldsymbol{y}$ with $\sigma = 0.26$, maximizing $\widehat{\rho}(1,1)$; (d) output $\boldsymbol{y}$ with $\sigma = 0.32$, maximizing Q; (e) output $\boldsymbol{y}$ with $\sigma = 0.24$, maximizing $CQ(1,1)$.